Int J Adv Manuf Technol
https://doi.org/10.1007/s00170-017-1309-7

ORIGINAL ARTICLE

Experimental diagnosis of broken rotor bars fault in induction machine based on Hilbert and discrete wavelet transforms

Hicham Talhaoui[1] · **Arezki Menacer**[2] · **Abdelhalim Kessal**[1] · **Ameid Tarek**[2]

Received: 16 June 2017 / Accepted: 1 November 2017

Abstract In this paper, a diagnosis method based on Hilbert and discrete wavelet transform (DWT) for broken rotor bars in induction machine has been proposed. The method is based from using Hilbert transform (HT) to obtain the envelope for the stator current and processed via DWT. The main advantage of HT is the removal of the fundamental component to allow a clearer vision of the fault frequencies. The result by HDWT (HT and DWT) is more suitable for emergency signal analysis. This technique is effective for the stationary signal as well as non-stationary signal processing. The HDWT analysis was introduced to overcome the shortcomings of Fourier analysis. The performance of this approach is evaluated in simulation and experimental results.

Keywords Induction machine · Broken rotor bars fault · Hilbert · Discrete wavelet

1 Introduction

Generally, induction machines are largely used in the electrical drives. These machines are characterized by good robustness, simple construction, low cost, and high efficiency. Although, all of these qualities, some constraints with a different nature can affect on the machine by causing failures in the stator and the rotor. Thereby, a sudden stop due to any anomaly can lead to financial losses (production losses, repair of the production tool…) and material losses inevitable. These breakdowns can be divided into two categories such as mechanical (defect on coupling, static and/or dynamic eccentricity, bearing failures…) [1, 2] or electrical and magnetic (inter-turn short circuit, broken rotor bars, break of teeth…) [3, 4].

Diverse techniques are largely investigated and applied for the fault detection in the machine. The first methods are founded on noise, temperature, and vibration analysis [5]. However, these methods are quite expensive and the mechanical installation is sensitive to the noise. The second technique, named motor current signature analysis (MCSA), the philosophy of this approach assumes that each type of defect is characterized by an own spectral signature. This method has some advantages like the simplicity of the current measuring and is based on straightforward signal processing techniques for example: fast Fourier transforms (FFT). The FFT is a good technique for the broken rotor bars fault detection in the steady state [6, 7]. However, it is often difficult to successfully detect the sideband frequencies due to the rapprochement and the overlap with the fundamental driving frequency. In order to overwhelm this problematic, the HT is recommended [8]. This last method has the best frequency, location for the DWT, which has been previously applied directly to the stator current for the broken rotor bars fault diagnosis in induction machine. In this case, the DWT is

✉ Abdelhalim Kessal
Abdelhalim.kessal@yahoo.fr

[1] LPMRN Laboratory, Faculty of Sciences and Technology, University of Bordj Bou Arreridj, Bordj Bou Arreridj, Algeria

[2] LGEB Laboratory, Department of Electrical Engineering, University of Biskra, Biskra, Algeria

Published online: 10 November 2017

used as an efficient time-domain algorithm which gives optimal precision at the short frequency and non-stationary state.

The WT is a recent signal processing tool for time-varying or non-stationary signals; it is based on the decomposition of a signal on a basis of particular functions. The wavelet analysis allows the use of long time intervals that require more precision in low frequencies and short regions for high frequencies. From this point of view, it is quite comparable to the Fourier analysis. However, wavelets are broadly oscillating functions that are rapidly damped, in contrast to the sinusoidal functions of Fourier analysis. Moreover, the wavelets possess the property of being able to be well localized in time or frequency, which differentiates them mainly from the conventional time-frequency analysis [9, 10].

In this context, the important goal of this paper is to present another technique for diagnosis of the fault in induction machines based on Hilbert and discrete wavelet transform analysis of stator current which would overwhelm the overarching problems of traditional FFT. A technique has been proposed based on the calculation of the energy stored in each level of decomposition (HDWT); the fault severity can also be identified through the eigenvalues of energies. As well a comparative study based on the two approaches for the analysis of the stator current in steady state is presented. Finally, the method has been verified by the experimental results for a healthy rotor and two broken rotor bars of the machine.

2 Hilbert transform

The Hilbert transform is a time-domain convolution of signal $x(t)$ with $\frac{1}{t}$ and can emphasize the local properties of $x(t)$, as follows [11, 12]:

$$H[x(t)] = \frac{1}{\pi}\int_{-\infty}^{+\infty}\frac{x(\tau)}{t-\tau}d\tau = x(t)^{*}\frac{1}{\pi t} \tag{1}$$

where t is time, $x(t)$is a time-domain signal, * is the convolution indicates, and $H[x(t)]$ is the Hilbert transform of $x(t)$.

3 Discrete wavelet transforms (DWT)

Assume $S = (S_1, S_2 \ldots S_n)$ (S *sampled signal*), the DWT decomposes it into several wavelet signals (an approximation signal a_n, and n detail signals d_j ($j \in [1, n]$)) [13, 14]. The frequencies of approximation and detail signals can be given by:

$$f(d_j) \in \left[2^{-(j+1)}f_s,\ 2^{-j}f_s\right] \tag{2}$$

$$f(a_n) \in \left[0,\ 2^{-(n+1)}f_s\right] \tag{3}$$

more concretely, f_s (samples/s): the sampling rate used for capturing S, the detail signal d_j contains the information concerning the signal components with frequencies included in the interval.

The energy eigenvalue for each frequency band is given by [15]:

$$E_j = \sum_{k=1}^{k=n}\left|D_{jk}(n)\right|^2 \tag{4}$$

such as j is the level of decomposition, n is the discrete wavelet decomposition time, and D is the magnitude at each discrete point of the wavelet coefficient of the signal in the corresponding frequency band.

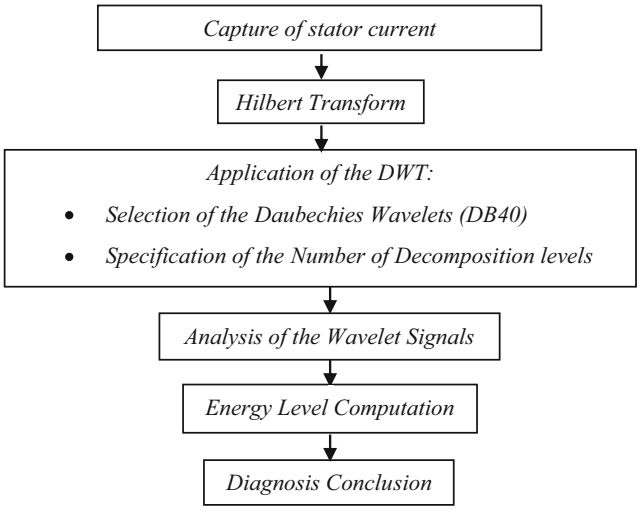

Fig. 1 The HDWT-based diagnosis methodology

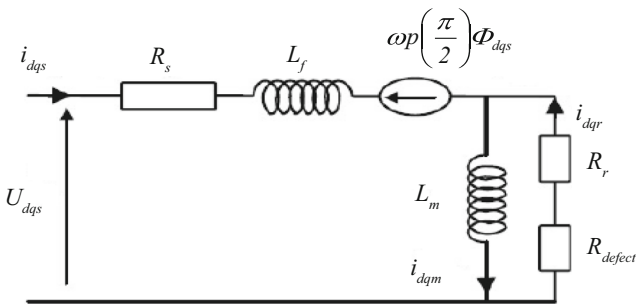

Fig. 2 Broken rotor bars model of induction machine

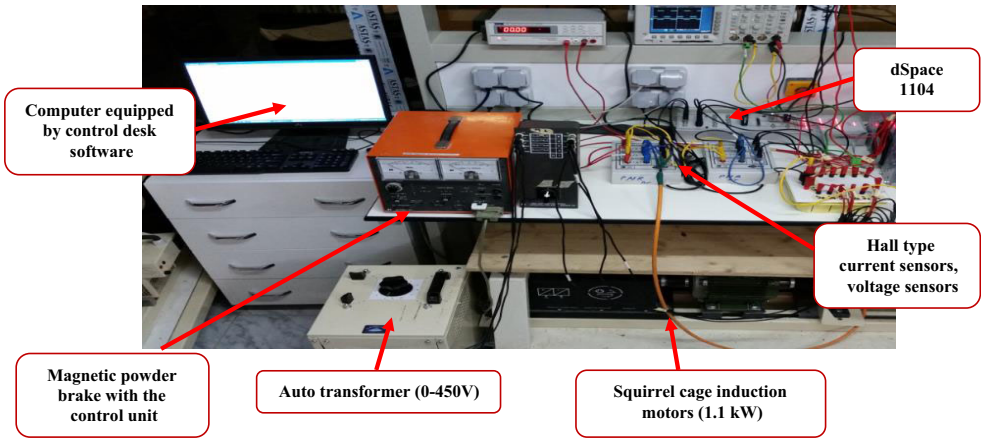

Fig. 3 Experimental setup

4 Fault diagnosis methodology

Figure 1 describes the steps that should be followed in order to apply the HDWT-based methodology for the diagnosis of rotor faults (broken rotor bars).

5 Model of induction machine taking account the broken rotor bars faults

Figure 2 shows the equivalent electrical diagram of induction machine with broken rotor bar's fault.

The state model of induction machine in the reference frame (d-q) related to the rotor can, therefore, be defined by the following system of nonlinear equations [7, 8]:

$$\begin{cases} \dot{x}(t) = A(\omega)x(t) + Bu(t) \\ y(t) = Cx(t) \end{cases} \tag{5}$$

with

$$[x] = [\,i_{ds} \quad i_{qs} \quad \Phi_{dr} \quad \Phi_{qr}\,]^T, \quad [u] = [U_{ds}, U_{qs}]^T, \quad [y] = [\,i_{ds} \quad i_{qs}\,]^T$$

$$A(\omega) = \begin{bmatrix} -(R_s + R_{eq})L_f^{-1} & \omega & R_{eq}L_m^{-1}L_f^{-1} & \omega L_f^{-1} \\ -\omega & -(R_s + R_{eq})L_f^{-1} & \omega L_f^{-1} & R_{eq}L_m^{-1}L_f^{-1} \\ R_{eq} & 0 & R_{eq}L_m^{-1} & 0 \\ 0 & R_{eq} & 0 & -R_{eq}L_m^{-1} \end{bmatrix}, \quad B = \begin{bmatrix} L_f^{-1} & 0 & 0 & 0 \\ 0 & L_f^{-1} & 0 & 0 \end{bmatrix}^T$$

$$C = \begin{bmatrix} 1 & 0 & 0 & 0 \\ 0 & 1 & 0 & 0 \end{bmatrix}; \quad Q(\theta_0) = \begin{bmatrix} \cos(\theta_0)^2 & \cos(\theta_0)\sin(\theta_0) \\ \cos(\theta_0)\sin(\theta_0) & \sin(\theta_0)^2 \end{bmatrix}, \quad R_{eq} = R_r + \frac{\alpha}{1-\alpha} Q(\theta_0) R_r$$

and $\alpha = \frac{2}{3}\eta_0$, $\eta_0 = \frac{3n_{bc}}{n_b}$, $\omega_r = \frac{\omega}{p}$: is mechanical speed of the motor.

n_{bc} and n_b represent the number of broken bars and the total number of bars in the rotor respectively.

θ_0 is an absolute localization of the faulty winding according to the first rotor phase.

The expression of the torque is defined by:

$$T_e = p\left(i_{qs}.\Phi_{dr} - i_{ds}.\Phi_{qr}\right) \tag{6}$$

6 Simulation and experimental results

The experimental setup (also for the simulated machine) used in this study consists of a 1.1 kW, 220/380 V, 50 Hz, rated current 2.5 A, four–pole, a DC generator acts as a load, and the experimental setup illustrated in Fig. (3). In the experimental test, the rotor bar breakage is realized by opening the motors and drilling in the rotor bar depth. In the experiments, the data acquisitions used are the voltage and stator current. The

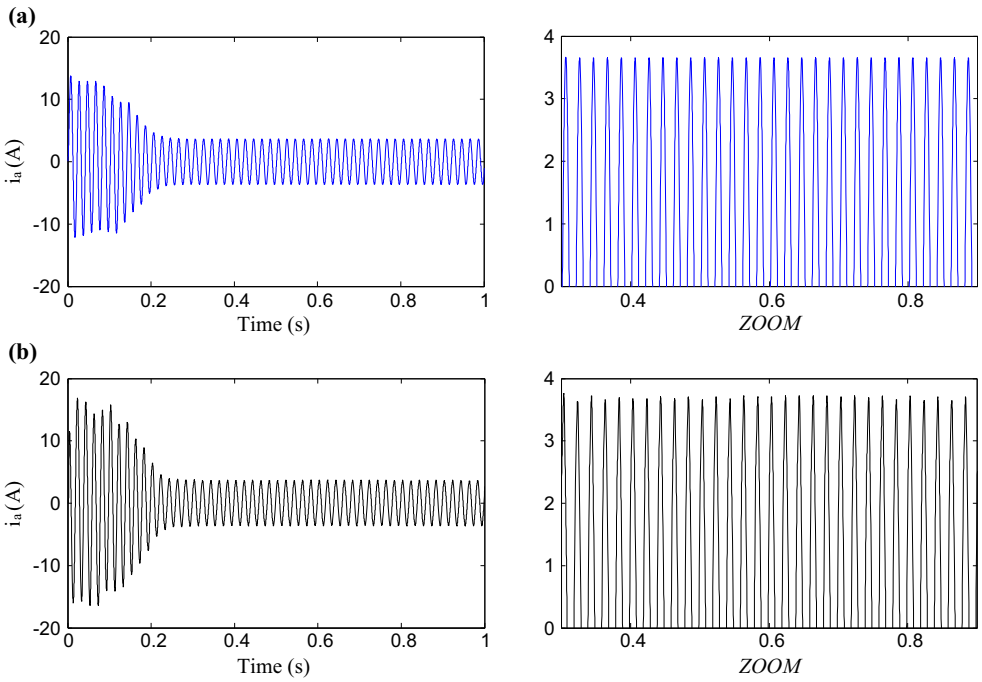

Fig. 4 Stator current for healthy machine. **a** Simulation results. **b** Experimental results

signals were connected to the computer by using DSpace (1104) for a data acquisition board.

In the experimental analysis, in order to wait good results and not to miss important information, it is important to take the acquisition information correctly. The motor current data was sampled at 10 kHz, i.e., 100,000 samples was obtained at a measured time of 10 s. All the signal processing was performed using MATLAB software.

The startup stator current waveforms for a loaded machine extracted by simulation and experimental tests are given in Figs. 4 and 5.

Figures 4 and 5 illustrate the stator current in a healthy and faulty state of the machine, respectively. The full load is applied at the start-up.

It is noted a good similarity between the results; the currents for the healthy and faulty state of the machine have a small modification.

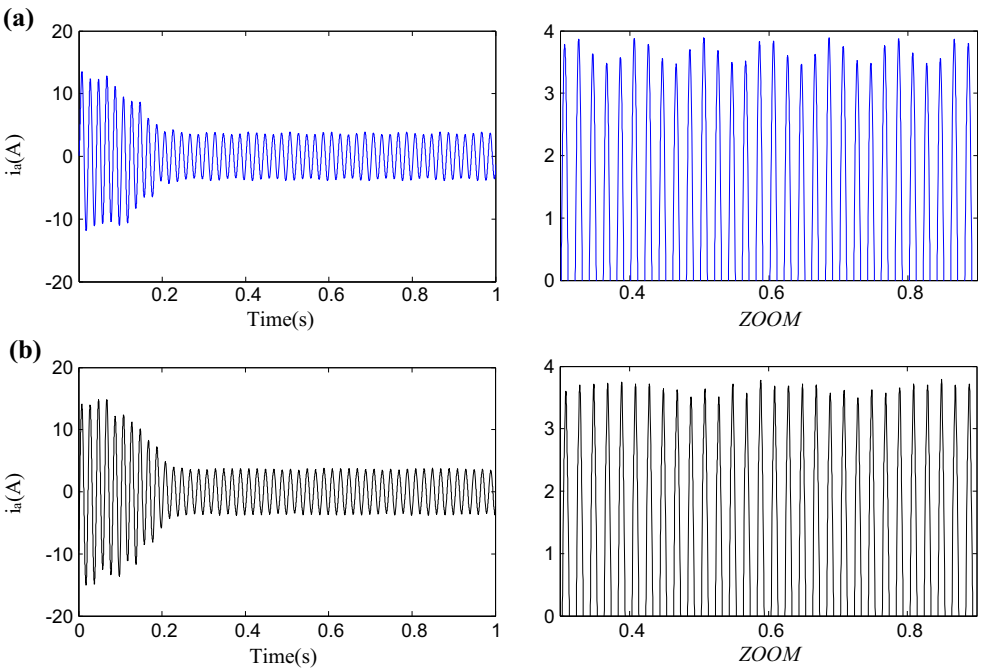

Fig. 5 Stator current for machine with two broken rotor bars. **a** Simulation results. **b** Experimental results

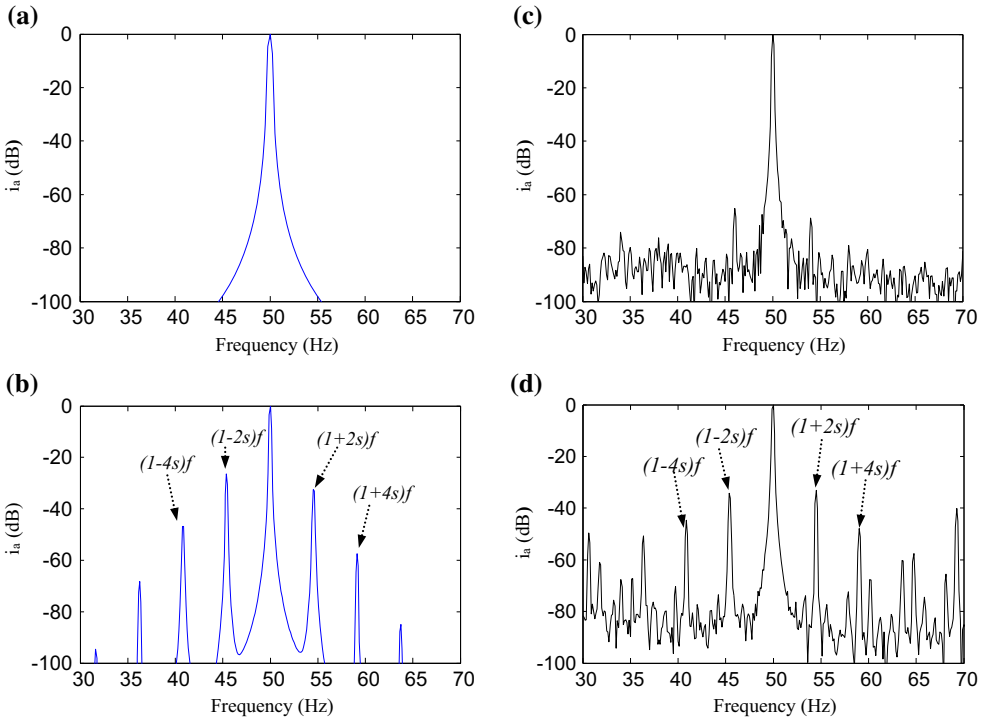

Fig. 6 FFT of stator current in steady state. **a**, **c** Healthy machine. **b**, **d** Machine with two broken rotor bars. **a**, **b** Simulation results. **c**, **d** Experimental results

The direct detection of the fault through the electrical characteristics is difficult. The frequency analysis of the signals, coming from the machine, gives a good prognosis of detection through the analysis of harmonics. If the number of broken rotor bars is augmented, an increase in the magnitude (of harmonics) is observed.

Figure 6a–d illustrates the result of the stator current analysis extracted in simulation and in experimental results for the machine at healthy and two broken rotor bars.

Figure 6a–d shows the frequency spectrum of the stator current around the network frequency of 50 Hz that is at [16]:

$$f_{defect} = (1 \pm 2ks)f \tag{7}$$

where $k = 1, 2, 3,...$, f is the frequency training of the machine, and s is the fractional slip of the motor.

It is also remarked that the calculated frequencies are almost similar from the deduced ones in the simulation and experimental (Tables 1 and 2).

Despite all these, there are several problems, especially at low load, this leads to difficulty in analyzing the fault because the frequency of defects is very close to the fundamental component. To overcome this difficulty, the amplitude modulation (AM) of the stator current induced is proposed. The harmonics contained in the spectrum of the stator current envelope can be written by the expression [17]:

$$f_{Hdefect} = 2ksf \tag{8}$$

The stator current envelope obtained for the healthy and two rotor broken bar conditions are shown in Fig. 7.

Figure 8a–d illustrates the result of frequency analysis of the stator current envelope.

From Fig. 8, it is observed then the stator current envelopes contain the information for the fault (broken rotor bars) through the characteristic harmonic components $2sf$, $4sf$ (in general "$2ksf$"). Tables (3 and 4) show that the values of deduced and calculated frequencies are similar.

The major disadvantage of this method is that, since the length of the window is fixed, it is not possible to simultaneously analyze phenomena whose time scales are different.

Table 1 Simulation frequencies and magnitudes of the stator current spectrum for the machine with two broken rotor bars

s = 4.5%	$(1-4s).f$	$(1-2s).f$	$(1+2s).f$	$(1+4s).f$
$f_{calculated}$ (Hz)	41	45.5	54.5	59
$f_{deduced}$ (Hz)	40.88	45.38	54.5	59.13
Magnitude (dB)	− 46.92	− 26.39	− 32.53	− 57.41

Table 2 Experimental frequencies and magnitudes of the stator current spectrum for the machine with two broken rotor bars

s = 4.5%	$(1-4s).f$	$(1-2s).f$	$(1+2s).f$	$(1+4s).f$
$f_{calculated}$ (Hz)	41	45.5	54.5	59
$f_{deduced}$ (Hz)	40.88	45.38	54.5	59
Magnitude (dB)	− 44.64	− 34 − 28	− 33.18	− 47.87

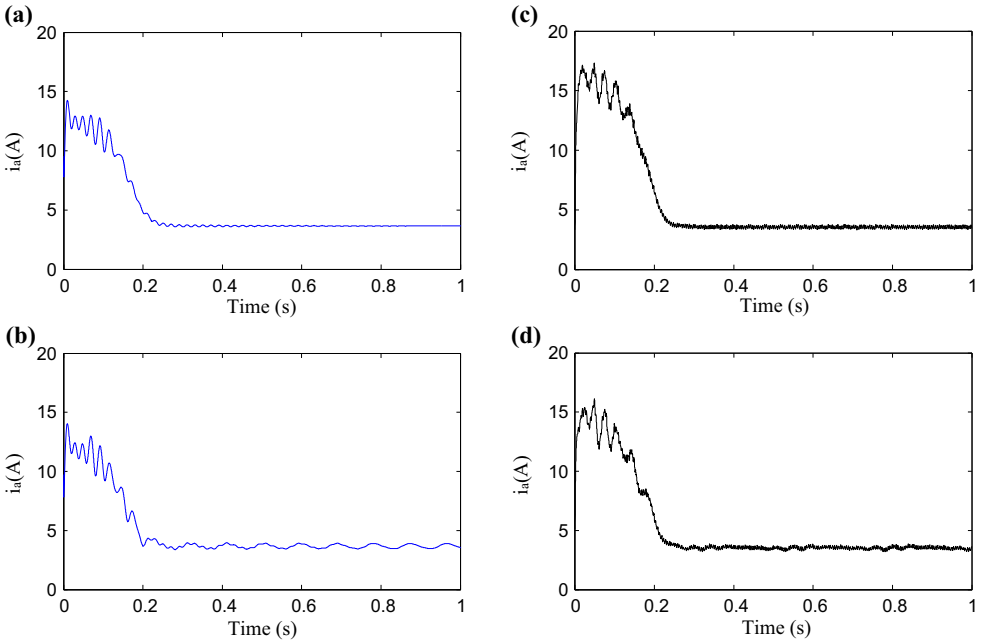

Fig. 7 Stator current envelope for **a**, **c** healthy machine, **b**, **d** machine with two broken rotor bars, **a**, **b** simulation results, and **c**, **d** experimental results

Another technique of analysis, which does not favor any particular scale, we propose DWT to eliminate this problem. The transformation by the wavelet technique is introduced with the aim of overcoming the difficulties mentioned above. A windowing technique with variable size is used to improve the analysis of the stator current signal in transient or permanent conditions.

The decomposition level n depends on the sampling rate f_s and on the frequency net f. It can be calculated by the expression [18]:

$$n > \frac{\log(f_s/f)}{\log(2)} + 1 \tag{9}$$

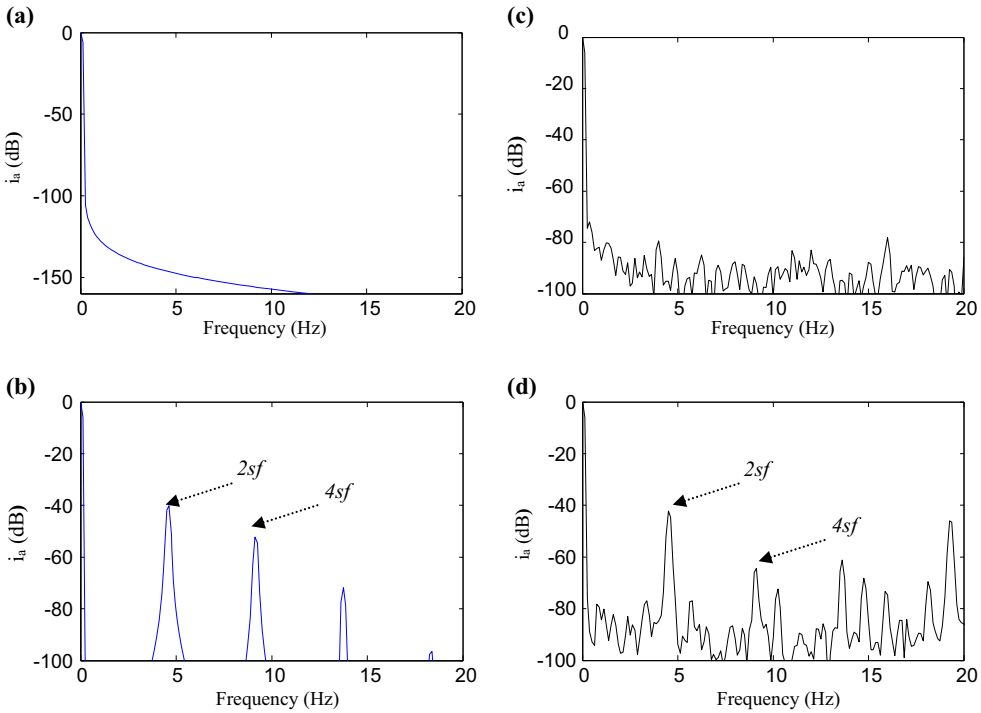

Fig. 8 FFT of spectrum of stator current envelope in steady state. **a**, **c** Healthy machine. **b**, **d** Machine with two broken rotor bars. **a**, **b** Simulation results. **c**, **d** Experimental results

Table 3 Simulation frequencies and magnitudes of the stator current envelope spectrum for the machine with two broken rotor bars

s = 4.5%	$2sf$	$4sf$
$f_{calculated}$ (Hz)	4.5	9
$f_{deduced}$ (Hz)	4.625	9.125
Magnitude (dB)	− 40 − 12	− 52.31

Table 4 Experimental frequencies and magnitudes of the stator current envelope spectrum for the machine with two broken rotor bars

s = 4.5%	$2sf$	$4sf$
$f_{calculated}$ (Hz)	4.5	9
$f_{deduced}$ (Hz)	4.5	9.125
Magnitude (dB)	− 42.3	− 64.51

Table 5 Frequency levels of wavelet coefficients

Level	Frequency band
a9	0–19.53 Hz
d9	19.53–39.06 Hz
d8	39.06–78.12 Hz
d7	78.12–156.25 Hz

the sampling rate of signals was f_s = 10,000 samples/s. The supply frequency in this paper is taken to be f = 50 Hz. Table 5 shows the frequency band for each level.

The "Daubechies (db) wavelets" of diverse order are used to decompose the stator current of each machine. Figure 9a–d, appearances that the upper-level signals (a9, d9, and d8) obtained by db40.

Although there are slight differences between the healthy and faulty state, it is difficult to know the fault because the frequency 50 Hz (the fundamental component) plays a role in this problem and it is existent in the complete analysis. To remove this problem, the Hilbert transform is presented to remove the fundamental component in both signals. In Figure 10, the DWT of the stator current envelope is displayed and the evolution in the observed frequency bands of the relative signal to the rotor defect can be analyzed using coefficients a9, d9, and d8.

Comparison of the detail and approximation signals for a machine with faults (broken rotor bars) shows that the amplitude of the coefficient a9 is increased relative to that in the case of to the healthy machine as they contain the frequency components $2sf$, where the field of frequency band is [0–19.53 Hz] (Table 5). The DWT, therefore, is a very effective tool for detecting the of broken rotor bars in a loaded machine.

Figure 11 shows the DWT of the stator current envelope at start-up sate given in Fig. 7.

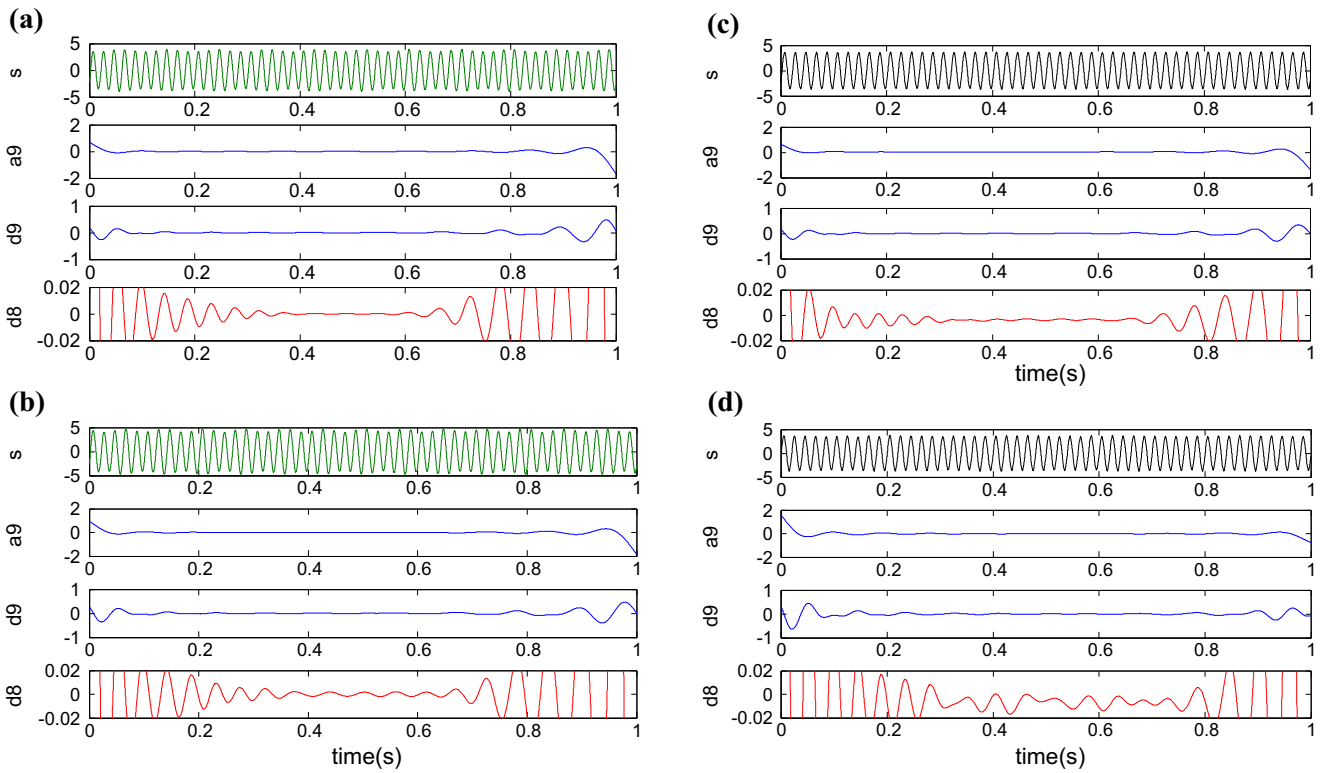

Fig. 9 DWT analysis of current stator. **a**, **c** Healthy machine. **b**, **d** Machine with two broken rotor bars. **a**, **b** Simulation results. **c**, **d** Experimental results

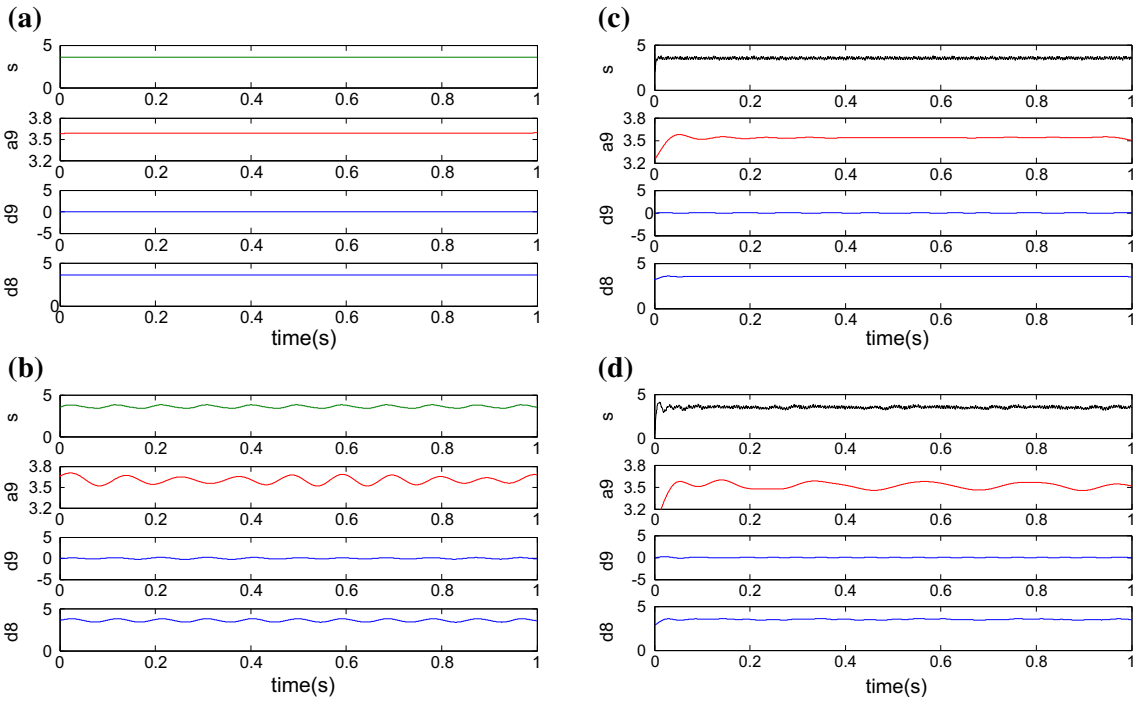

Fig. 10 DWT analysis of current stator envelope. **a**, **c** Healthy machine **b**, **d** Machine with two broken rotor bars. **a**, **b** Simulation results. **c**, **d** Experimental results

Through Fig. 11b, it is noticed that the removal of the fundamental has a very significant effect on the diagnosis of defaults. This effect is deduced by the variation in the amplitudes of the signals in bands a9, in the faulty state compared with a healthy state.

In Fig. 12, the simulation and experimental results show the variation of the energy in the frequency bands of decomposition of the wavelet for the healthy and faulty state.

The calculation of the energy stored in each decomposition level confirms the increase observed in the detail and

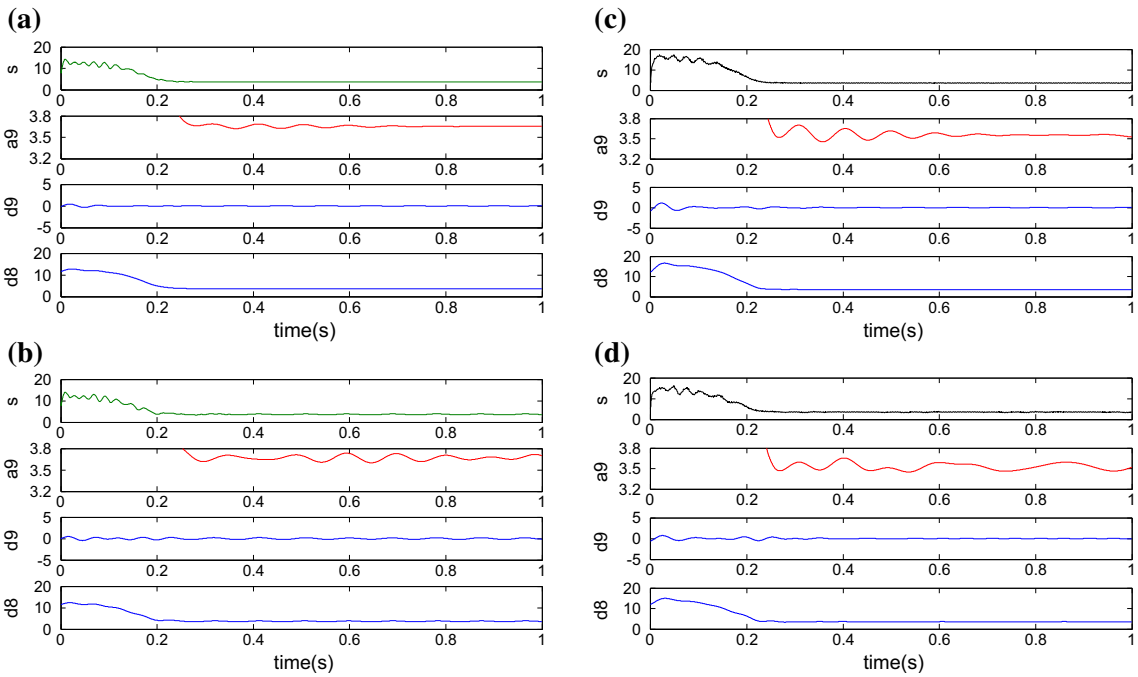

Fig. 11 DWT analysis of current stator envelope (startup state with full load). **a**, **c** Healthy machine. **b**, **d** Machine with two broken rotor bars. **a**, **b** Simulation results. **c**, **d** experimental results

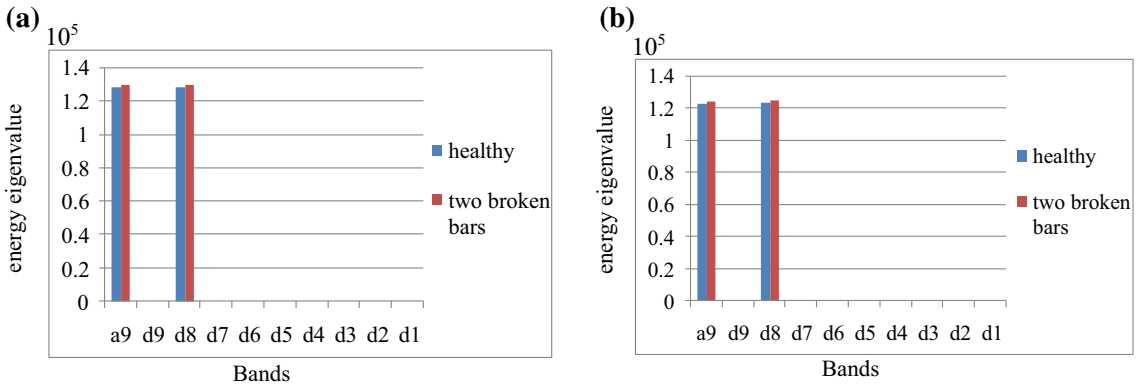

Fig. 12 Eigenvector changes at various levels of decomposed signals. **a** Simulation results. **b** Experimental results

approximation signals, especially in the level E8 (d8) (even for a9), which indicates the energy of this frequency band, can be a suitable criterion to detect the broken bars.

7 Conclusion

In this paper, a good method for broken rotor bar detection and diagnosis in induction machine is proposed. The method is based on Hilbert and discrete wavelet transform. The result obtained from analysis of the stator current in simulation and experimental shows the existence of a defect through the different harmonic's appearance in the spectrum. However, there are several problems, especially at low load, this leads to difficulty in analyzing the fault because the frequency of defects are very close to the fundamental component. The envelope analysis, with the help of the Hilbert transform produced quite satisfactory results. The elimination of the fundamental component allows a clearer identification of the fault frequencies. The results obtained by using FFT (even for Hilbert) analysis in a steady state have been proved to be a very effective method for stationary system and have been widely used in the monitoring, fault detection, and diagnosis in the industry. Hence, the complementary collaboration of wavelet transformation is required. The results obtained by the HDWT give the advantageous information to decide the faulty situation, particularly in the presence of broken rotor bars at start-up. The HDWT is also used for calculation of the energy stored in each level of decomposition (HDWT); the degree of the defect can also be identified through the eigenvalues of energies. The energy eigenvalue offers a good sign for the detection of the rotor fault at low load and non-stationary state. Simulation and experimental results confirm the efficiency of the proposed approach, which can be extended for the detection of the rotor fault (broken bar) for other types of induction machine; where this method has not related to the power of the machine.

Nomenclature k, integer; U_d, U_q, instantaneous voltage d; q components (Park); i_d, i_q, instantaneous current d; q components (Park); Φ_d, Φ_q, instantaneous flux d; q components (Park); ω_r, electrical speed of the rotor in rad/sec; T_e, electromagnetic torque; s, motor slip; R_s, stator resistance; R_r, rotor resistance; L_m, mutual inductance; L_f, leakage inductance of stator; p, number of pole pairs; n_b, number of rotor bars; n_s, number of turns per stator phase; θ_0, absolute localization of the faulty winding according to the first rotor phase; i_a, instantaneous current (a) component (stator phase (a)); a_n, approximation signal and n detail signals d_j; d_j, detail signal ($j \in [1, n]$); S, sampled signal

References

1. Talhaoui H, Menacer A, Kechida R (2015) Mixed eccentricity fault diagnosis in the sensorless field oriented control induction motor using DWT technique. Diagnostics Electr Mach Power Electron Drives (SDEMPED), 2015 I.E. 10th Int Symp 97–103. https://doi.org/10.1109/DEMPED.2015.7303675
2. Kedadouche M, Liu Z, V-H V (2016) A new approach based on OMA-empirical wavelet transforms for bearing fault diagnosis. Measurement 90:292–308. https://doi.org/10.1016/j.measurement.2016.04.069
3. Guezmil A, Berriri H, Pusca R et al (2017) Detecting inter-turn short-circuit fault in induction machine using high-order sliding mode observer: simulation and experimental verification. J Control Autom Electr Syst. https://doi.org/10.1007/s40313-017-0314-2
4. Ameid T, Menacer A, Talhaoui H, Harzelli I (2017) Broken rotor bar fault diagnosis using fast Fourier transform applied to field-oriented control induction machine: simulation and experimental study. Int J Adv Manuf Technol. https://doi.org/10.1007/s00170-017-0143-2
5. Gyftakis KN, Spyropoulos DV, Kappatou JC, Mitronikas ED (2013) A novel approach for broken bar fault diagnosis in induction motors through torque monitoring. IEEE Trans Energy Convers 28:267–277. https://doi.org/10.1109/TEC.2013.2240683
6. Aydin I, Karakose M, Akin E (2011) A new method for early fault detection and diagnosis of broken rotor bars. Energy Convers Manag 52:1790–1799. https://doi.org/10.1016/j.enconman.2010.11.018
7. Kechida R, Menacer A, Talhaoui H (2013) Approach signal for rotor fault detection in induction motors. J Fail Anal Prev 13:346–352. https://doi.org/10.1007/s11668-013-9681-6
8. Bessam B, Menacer A, Boumehraz M, Cherif H (2015) DWT and Hilbert transform for broken rotor bar fault diagnosis in induction

machine at low load. Energy Procedia 74:1248–1257. https://doi.org/10.1016/j.egypro.2015.07.769
9. Kia SH, Henao H, Capolino G-A (2009) Diagnosis of broken-bar fault in induction machines using discrete wavelet transform without slip estimation. IEEE Trans Ind Appl 45:1395–1404. https://doi.org/10.1109/TIA.2009.2018975
10. Bouzida A, Touhami O, Ibtiouen R et al (2011) Fault diagnosis in industrial induction machines through discrete wavelet transform. IEEE Trans Ind Electron 58:4385–4395. https://doi.org/10.1109/TIE.2010.2095391
11. Oumaamar MEK, Razik H, Rezzoug A, Khezzar A (2013) Line current analysis for bearing fault detection in induction motors using Hilbert transform phase. Int Aegean Conf Electr Mach Power Electron Electromotion Jt Conf 2:288–293. https://doi.org/10.1109/ACEMP.2011.6490612
12. Yang DM (2012) Induction motor bearing fault diagnosis using hilbert-based bispectral analysis. Proc-2012 Int Symp Comput Consum Control IS3C 2012 385–388. https://doi.org/10.1109/IS3C.2012.104
13. Yahia K, Cardoso AJM, Ghoggal A, Zouzou SE (2014) Induction motors airgap-eccentricity detection through the discrete wavelet transform of the apparent power signal under non-stationary operating conditions. ISA Trans 53:603–611. https://doi.org/10.1016/j.isatra.2013.12.002
14. Singh M, Yadav RK, Kumar R (2013) Discrete wavelet transform based measurement of inner race defect width in taper roller bearing. Mapan 28:17–23. https://doi.org/10.1007/s12647-013-0045-1
15. Kapoor SR, Khandelwal N, Pareek P (2014) Bearing fault analysis by signal energy calculation based signal processing technique in squirrel cage induction motor. In: 2014 Int Conf Signal Propag Comput Technol (ICSPCT 2014) IEEE, pp 33–38
16. Ameid T, Menacer A, Talhaoui H, Harzelli I (2017) Rotor resistance estimation using extended Kalman filter and spectral analysis for rotor bar fault diagnosis of sensorless vector control induction motor. Measurement 111:243–259. https://doi.org/10.1016/j.measurement.2017.07.039
17. Bessam B, Menacer A, Boumehraz M, Cherif H (2016) Detection of broken rotor bar faults in induction motor at low load using neural network. ISA Trans 64:241–246. https://doi.org/10.1016/j.isatra.2016.06.004
18. Talhaoui H, Menacer A, Kessal A, Kechida R (2014) Fast Fourier and discrete wavelet transforms applied to sensorless vector control induction motor for rotor bar faults diagnosis. ISA Trans 53:1639–1649. https://doi.org/10.1016/j.isatra.2014.06.003